



Contents lists available at ScienceDirect

Archives of Biochemistry and Biophysics

journal homepage: www.elsevier.com/locate/yabbi

Simultaneous measurement of CYP1A2 activity, regioselectivity, and coupling: Implications for environmental sensitivity of enzyme–substrate binding

Matthew J. Traylor, Jack Chai, Douglas S. Clark*

Department of Chemical and Biomolecular Engineering, University of California, Berkeley, CA 94720, United States

ARTICLE INFO

Article history:

Received 25 August 2010
and in revised form 4 October 2010
Available online 8 October 2010

Keywords:

P450 regioselectivity
P450 coupling
CYP1A2
Cyanocoumarin

ABSTRACT

The cytochrome P450 (CYP) reaction mechanism often yields a broad array of coupled and uncoupled products from a single substrate. While it is well known that reaction conditions can drastically affect the rate of P450 catalysis, their effects on regioselectivity and coupling are not well characterized. To investigate such effects, the CYP1A2 oxidation of 7-ethoxymethoxy-3-cyanocoumarin (EOMCC) was examined as a function of buffer type, buffer concentration, pH, and temperature. A high-throughput, optical method was developed to simultaneously measure the rate of substrate depletion, NADPH depletion, and generation of the O-dealkylated product. Increasing the phosphate buffer concentration and temperature increased both the NADPH and EOMCC depletion rates by 6-fold, whereas coupling was constant at 7.9% and the regioselectivity of O-dealkylation to other coupled pathways was constant at 21.7%. Varying the buffer type and pH increased NADPH depletion by 2.5-fold and EOMCC depletion by 3.5-fold; however, neither coupling nor regioselectivity was constant, with variations of 14.4% and 21.6%, respectively. Because the enzyme–substrate binding interaction is a primary determinant of both coupling and regioselectivity, it is reasonable to conclude that ionic strength, as varied by the buffer concentration, and temperature alter the rate without affecting binding while buffer type and pH alter both.

© 2010 Elsevier Inc. All rights reserved.

Introduction

Human cytochrome P450¹ enzymes are important to the pharmaceutical and biotechnology industries due to their central role in drug metabolism, ability to generate and optimize lead compounds, and specialized oxidative abilities [1]. The use of P450 enzymes in these capacities is complicated, however, by the wide variability of reaction rates observed in reconstituted *in vitro* systems [2,3]. This variability has been linked to the composition of the reaction medium [4–7]. Because the P450 reaction mechanism is capable of generating multiple products, it is not known whether the variability in rates as a function of medium composition is accompanied by significant changes in selectivity.

Multiple P450 reaction products comprise two classes: coupled products where the electrons supplied by NADPH are coupled to

substrate oxidation, and uncoupled products where the supplied electrons are lost to reduced oxygen species [8]. Thus, there are two relevant reaction selectivities in P450 systems: the electron selectivity, commonly referred to as the coupling efficiency, which is the ratio of coupled to uncoupled product-generation rates; and the regioselectivity, which is the ratio of two different possible coupled product-generation rates. While it is well known that reaction conditions can affect P450 activity over orders of magnitude [6], it is currently unclear how P450 enzymes interact with environmental parameters such as pH, ionic strength, temperature, and small molecule additives to modulate these two selectivities. An improved understanding of these interactions could lead to more accurate *in vitro* – *in vivo* metabolic correlations facilitating drug development [3], and assist in the development and optimization of synthetic schemes in the biotechnology sector [2,9].

P450 regioselectivity is thought to be controlled by a combination of substrate positioning with respect to the active oxidant and the relative reactivity of different potential oxidation sites on the substrate [10]. Regioselectivity of a very mobile substrate, one able to bind in many orientations, is likely governed primarily by the relative reactivity of the different chemical moieties in proximity to the heme. In contrast, regioselectivity of a tightly-bound substrate, one able to bind in only a few orientations, is presumably determined primarily by the relative occupancy of the different binding orientations [11,12]. Thus, an experimental parameter that

* Corresponding author. Fax: +1 510 643 1228.

E-mail address: clark@berkeley.edu (D.S. Clark).

¹ Abbreviations used: 7HCC, 7-hydroxy-3-cyanocoumarin; CYP, cytochrome P450; P450, cytochrome P450; EOMCC, 7-ethoxymethoxy-3-cyanocoumarin; PBO, piperonyl butoxide; NADPH, nicotinamide adenine dinucleotide phosphate; LCMS, liquid chromatography tandem mass spectrometry; MS/MS, tandem mass spectrometry; r_{7HCC} , initial rate of 7-hydroxy-3-cyanocoumarin generation; $-r_{EOMCC}$, initial rate of 7-ethoxymethoxy-3-cyanocoumarin depletion; $-r_{NADPH}$, initial rate of nicotinamide adenine dinucleotide phosphate depletion; HEPES, 4-(2-hydroxyethyl)-1-piperazineethanesulfonic acid; RFU, relative fluorescence units.

alters regioselectivity would be expected to modify the occupancy or orientation of different binding modes of the substrate or differentially modify the reactivity of the substrate. The latter has been clearly demonstrated in kinetic isotope effect studies where the substitution of a heavy atom at one oxidation site of a mobile substrate can alter the regioselectivity toward reaction at other sites [13]. Although previous studies have investigated the effect of buffer concentration, pH, and magnesium concentration on the regioselectivity of P450 reactions, the regulation of P450 selectivity by reaction conditions remains poorly understood. Buffer and magnesium concentrations have been found to alter catalytic activity but not regioselectivity, while pH has been shown to alter both [14–17].

Electron selectivity, or coupling, has also been linked to substrate–enzyme binding interactions. The structural complementarity of the substrate and P450 active site has been shown to be an important determinant of coupling [18,19], where noncomplementarity results in improperly positioned water in the active site. These water molecules are thought to disrupt the proton delivery machinery required for the successive protonation of the ferric-peroxo intermediate, leading to a decrease in coupling efficiency [20]. Guengerich points out that substrate dissociation rates can be large compared to catalytic rates, and coupling efficiency can be decreased by substrate dissociation after initiation of catalysis but before oxidation [21]. Thus, a parameter that modifies the substrate–enzyme interaction and alters the off-rate or the packing of the active site is expected to affect coupling. Notably, an increase in buffer concentration was shown to increase coupling in the benzphetamine N-demethylation activity of CYP2B4 enriched rabbit liver microsomes [22]; however, there are few studies in the literature examining the effect of reaction conditions on uncoupling.

In general, very little has been published on the relationship between environment and P450 selectivity. In particular, no previous studies have investigated the effect of reaction conditions on CYP1A2 regioselectivity or coupling. This void in the literature can be partially attributed to the large number of measurements needed to calculate these selectivities. To address this limitation, we developed a “one pot” method utilizing a single experimental technique, fluorescence intensity measurements, to simultaneously quantify activity, regioselectivity, and coupling. Depletion rates of NADPH and of an optically active substrate are analyzed in concert with the generation rate of at least one product. This method should be generally applicable to any substrate that is optically distinguishable from NADPH and one or more of its products. Here the method is demonstrated with the CYP1A2 oxidation of EOMCC to 7-hydroxy-3-cyanocoumarin (7HCC), which is a particularly challenging case study because the substrate’s fluorescence spectrum overlaps with the spectrum of NADPH. In addition, due to the broad reactivity of cyanocoumarins [23], this model reaction can be used for many human drug metabolizing P450 enzymes allowing for a more direct comparison of selectivity data between isozymes.

To explore the relationship between environment and selectivity, the rates of NADPH depletion, EOMCC depletion, and 7HCC generation were measured as a function of buffer type, buffer concentration, pH, and temperature in the CYP1A2 oxidation of EOMCC, and the regioselectivity and coupling were compared under these conditions. The results indicate that both regioselectivity and coupling remain constant when temperature and buffer concentration are varied but are altered when buffer type and pH are varied. This indicates that temperature and ionic strength, as varied by buffer concentration, affect the rate of catalysis independent of the substrate–enzyme binding interaction while pH and buffer type affect both the rates and the binding interaction.

Materials and methods

Materials

Piperonyl butoxide (PBO), potassium phosphate, nicotinamide adenine dinucleotide phosphate (NADPH), and acetonitrile were purchased from Sigma (St. Louis, MO). Microsomes from baculovirus-infected insect cells (Baculosomes) expressing human CYP1A2 and rabbit cytochrome P450 reductase (Lot 484429C), EOMCC, and 7HCC were purchased from Invitrogen (Carlsbad, Ca). All chemicals were used as received. All fluorescence data were acquired on a Spectramax M2 plate reader (Molecular Devices, Sunnyvale, CA).

Liquid chromatography mass spectrometry

EOMCC oxidation reactions were conducted in 120 mM pH 8 potassium phosphate buffer with 25 nM CYP1A2 Baculosomes with or without the inhibitor PBO. Reactions were initiated with the simultaneous addition of NADPH and EOMCC to a concentration of 450 μ M and 100 μ M, respectively, to a final volume of 200 μ L. Reactions were prepared and conducted at ambient temperature for 1 h and were quenched with 100 μ L ice cold acetonitrile then centrifuged at 4 °C for 10 min at 14,000g. Products were resolved using a reverse-phase Alltech Prevail C18 3 μ m 3.0 \times 150 mm column with a 0.4 ml/min flow rate and a gradient of 10–80% acetonitrile over 40 min with a constant 0.05% concentration of formic acid. LCMS data were collected on an Agilent 1100 LC/MSD equipped with an electrospray ion source. Injections of inhibited, uninhibited, and no-protein control reactions were conducted separately in positive and negative mode. The quadrupole ion analyzer MS was operated with a fragmentor setting of 70 V, 3 kV capillary, 35 psig nebulizer pressure, and with N₂ drying gas set to 300 °C and 9.5 L/min. LCMS/MS spectra were acquired using a ThermoFisher Scientific LTQ Orbitrap XL mass spectrometer in positive and negative modes. The flow rate was 0.2 mL/min and the mass spectrometer source parameters were used as follows: spray voltage, 3.0 kV; capillary temperature, 275 °C; capillary voltage, 44 V (positive mode) and –50 V (negative mode); tube lens, 125 V (positive mode) and –120 V (negative mode).

Activity and selectivity assays

Six replicates were prepared with 25 nM CYP1A2 Baculosomes at the buffer condition noted in Fig. 4 with and without 1 mM PBO. NADPH solutions were prepared fresh daily and the concentration was checked via absorbance using a molar extinction coefficient of 6.22 $\text{mM}^{-1}\text{cm}^{-1}$. Reactions were incubated for 20 min at the required temperature before initiation with the simultaneous addition of NADPH and EOMCC to 250 μ M and 10 μ M, respectively to a final volume of 100 μ L.

The reaction was followed via fluorescence intensity measurements in a Spectramax M2 plate reader. Fluorescence intensity was simultaneously recorded at three excitation/emission wavelengths: 340 nm/460 nm, 340 nm/520 nm, 409 nm/460 nm. Models correlating fluorescence intensity with the concentration of EOMCC, NADPH, and 7HCC (Eqs. (1)–(3)) were generated in JMP 5.1 using least-squares regression. The coefficients of Eqs. (1)–(3) were determined using on-plate standards at each reaction condition tested. The on-plate standards included a three-level, full factorial array of mixtures of NADPH and EOMCC to quantify fluorescence interactions. Significant model parameters were identified with the Backward Elimination method using a threshold *P*-value of 5%. Correlations typically took the form shown below.

$$\text{RFU}_{340/460} = a_1[\text{EOMCC}] + b_1[\text{EOMCC}][\text{NADPH}] + c_1[\text{NADPH}] + d_1[7\text{HCC}] \quad (1)$$

$$\text{RFU}_{340/520} = a_2[\text{NADPH}] + b_2[\text{NADPH}]^2 + c_2[\text{EOMCC}] + d_2[\text{NADPH}][7\text{HCC}] + e_2[7\text{HCC}] \quad (2)$$

$$\text{RFU}_{409/460} = a_3[7\text{HCC}] \quad (3)$$

The three coupled algebraic equations representing the dependence of fluorescence intensity on fluorophore concentration at each wavelength were solved for each data point in Matlab to yield concentration trajectories with time. The background reactions including PBO were subtracted out at each condition. The corrected time trajectory data were fit with a monoexponential function from which initial rates were calculated.

Results

Simultaneous *in situ* monitoring of EOMCC, 7HCC, and NADPH

The quantification of NADPH, EOMCC, and 7HCC via fluorescence intensity measurements is complicated in this system by the overlap of the fluorescence spectra of EOMCC and NADPH. While the emission of 7HCC is not affected by the presence of the other fluorophores, the emission maximum of NADPH (460 nm) overlaps with a strong signal from EOMCC (Fig. 1). However, at longer emission wavelengths, the NADPH signal is more distinct from that of the other fluorophores. The incorporation of emission data from both 460 nm and 520 nm upon excitation at 340 nm into a standard least-squares regression algorithm allowed

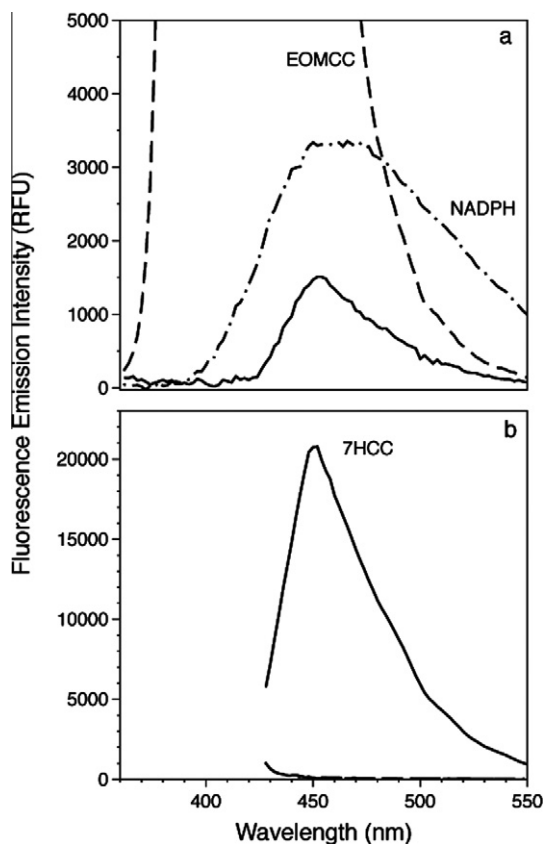


Fig. 1. Emission spectra of 250 μM NADPH, 10 μM EOMCC, and 1.2 μM 7HCC in 100 mM potassium phosphate at pH 7.5 upon excitation at (a) 340 nm and (b) 409 nm.

for the generation of models correlating fluorescence intensity with fluorophore concentration. Correlation parameters were determined using on-plate standards at each condition tested and were validated by comparing the predicted and measured fluorescence intensities for mixtures of known concentrations of fluorophores, each yielding R^2 values greater than 0.98 indicating accurate fluorophore quantification (data not shown).

These correlation equations were solved to yield each fluorophore concentration as a function of time. Representative time trajectories of the three fluorophore concentrations are shown in Fig. 2 for reactions with and without the P450 suicide inhibitor, PBO. Inhibition by PBO is hypothesized to occur via the formation of a stable carbene linkage to the heme iron blocking further catalysis by the P450 [24]. Degradation of EOMCC and NADPH occurs in the presence of PBO, which can be attributed to both the instability of these molecules and to reactions with other components of the heterogeneous baculosome mixture. The background response of the inhibited system, which contains all components except functional P450, is thus crucial to isolate the contribution of only CYP1A2 from other reactions occurring in the system, such as the background oxidation of NADPH by the reductase. The absence of any 7HCC generation in the presence of PBO also indicates that, within the reaction mixture, only functional CYP1A2 can catalyze the conversion of EOMCC to 7HCC. Monoexponential fits were applied to the corrected time trace data and initial rates were calculated for the degradation of EOMCC, the generation of 7HCC, and the degradation of NADPH. The exponential fit does not imply a mechanistic interpretation and was used because it closely reproduces the observed data (Fig. 2). Coupling is reported as the ratio of EOMCC depletion to NADPH depletion, and regioselectivity is indicated by the ratio of 7HCC generation to EOMCC depletion. A table of all measured rates and calculated selectivities can be found in the Supplemental materials.

Multiple coupled products in the CYP1A2 oxidation of EOMCC

To verify that the measured regioselectivity is governed by an enzyme-mediated process and not simply the rearrangement of a common intermediate into multiple products [25], the reaction profile was investigated with mass spectrometry. The reaction products of the CYP1A2 oxidation of EOMCC were analyzed with LCMS in the presence and absence of PBO. Product peaks were identifiable from background peaks as the product peaks disappeared in the presence of PBO. This was seen in three peaks eluting at 18.9 min, 23.6 min, and 30.5 min, which yielded major ions at m/z +236, -186, and -207, respectively (Fig. 3). Although the peak at 30.5 min exhibited a base peak at m/z -207, another product ion was present in this peak at a much lower abundance at m/z -234. EOMCC eluted at 33.4 min and as expected exhibited a larger peak with PBO than in its absence. The substrate peak co-eluted with an EOMCC standard while the product at 23.6 min co-eluted with a 7HCC standard (data not shown). The small peak at 33.4 min in the m/z -186 chromatogram (Fig. 3b) arises from fragmentation of the substrate EOMCC during ionization.

To determine whether CYP1A2 oxidizes EOMCC at multiple sites, LCMS/MS analysis was conducted on EOMCC, 7HCC, and the unknown m/z +236 product. Unfortunately, the m/z -234 product could not be captured with LCMS/MS. Mass spectra, exact mass data, chemical formula predictions, and spectra interpretation are provided in the Supplemental materials. The loss of 30 amu followed by 26 amu was identified in EOMCC as a fragmentation motif indicating the sequential loss of formaldehyde and ethylene from the 7-ethoxymethoxy moiety of the substrate. This motif was also seen in the fragmentation of the unknown m/z +236 product, demonstrating an intact 7-ethoxymethoxy moiety. The O-dealkylation of this moiety generates 7HCC; therefore, it can be

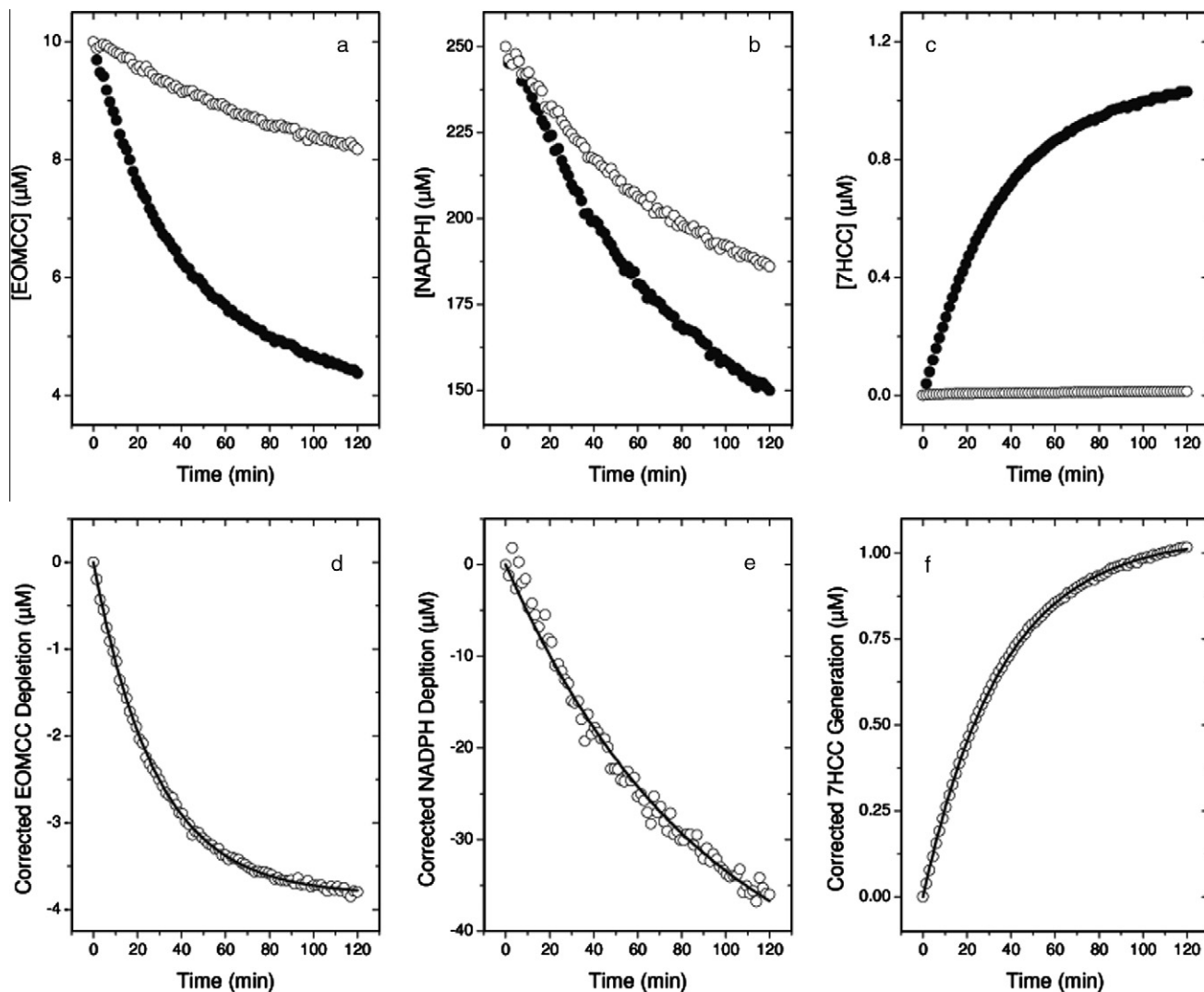


Fig. 2. Representative data for the depletion of EOMCC (a) and NADPH (b), and the generation of 7HCC (c), in the presence (○) and absence (●) of the inhibitor PBO. The data with inhibition are subtracted from the data without inhibition to yield the corrected depletion of EOMCC (d), NADPH (e), and generation of 7HCC (f). A monoexponential curve is fit to the data and used to obtain an initial rate.

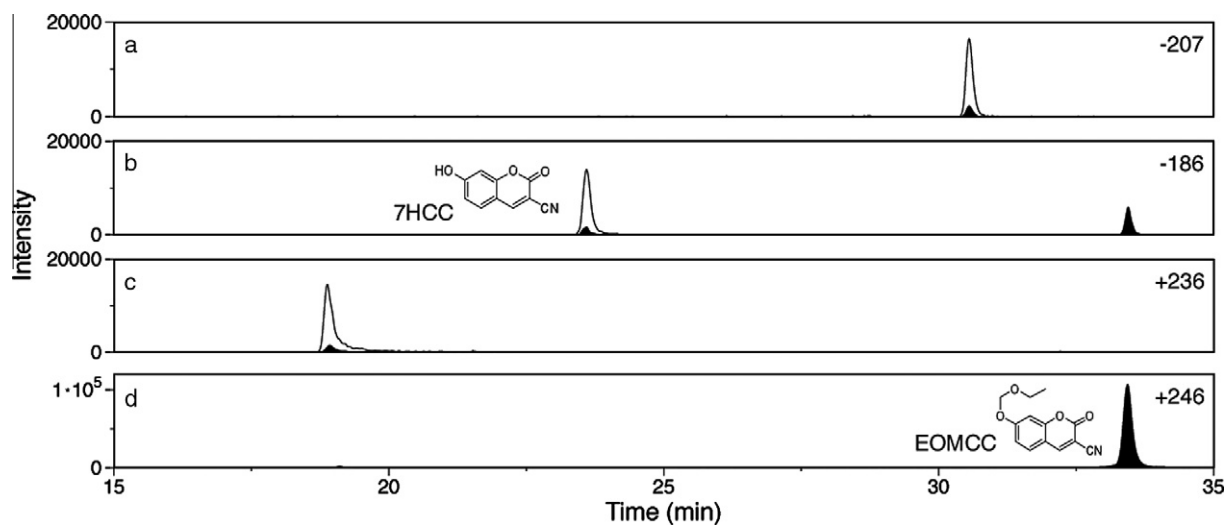


Fig. 3. LCMS analysis of the reaction products of the CYP1A2 oxidation of EOMCC with single ion monitoring in negative mode of (a) m/z -207 and (b) m/z -186 and in positive mode of (c) m/z +236 and (d) m/z +246. The filled peaks are data from reactions including the suicide inhibitor, PBO, while the empty peaks are the response without inhibitor.

concluded that the m/z +236 product is generated from the oxidation of EOMCC at a different site than 7HCC. Thus, EOMCC occupies at least two binding orientations in the CYP1A2 active site with at least two sites of oxidation on the substrate.

Effect of reaction conditions on activity and selectivity

The initial rates of 7HCC generation (r_{7HCC}), EOMCC depletion ($-r_{EOMCC}$), and NADPH depletion ($-r_{NADPH}$) were measured in the reaction of CYP1A2 on EOMCC as a function of buffer type, buffer concentration, pH, and temperature (Fig. 4). Each rate increased with temperature, and appeared to be approaching a maximum at the highest achievable temperature of 45 °C. Each rate also exhibited a maximum at a phosphate buffer concentration between 250 and 375 mM. A notable difference in rate was apparent, however, when varying the buffer type and pH, where $-r_{EOMCC}$ and $-r_{NADPH}$ both showed qualitatively similar behavior in Tris and phosphate

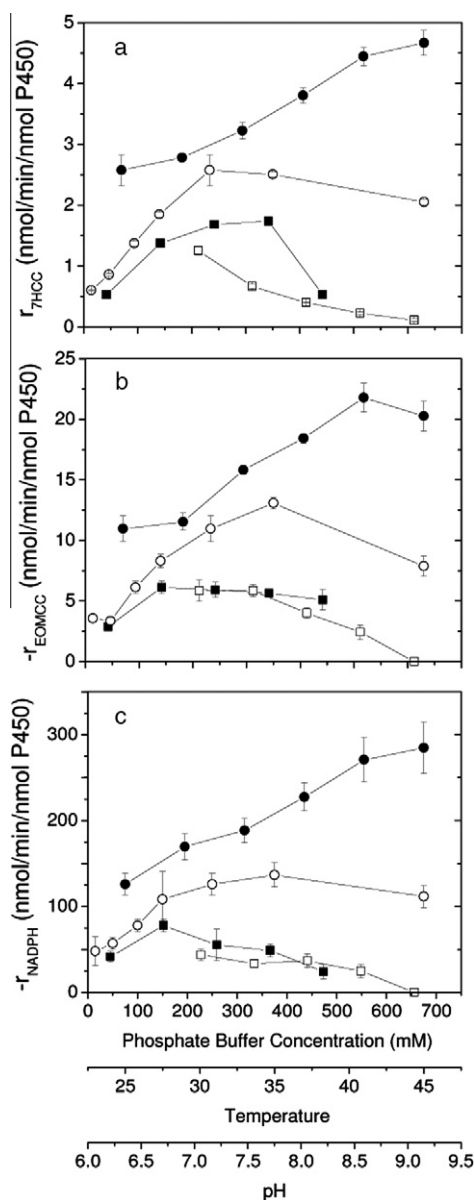


Fig. 4. Initial rates of (a) 7HCC generation, (b) EOMCC depletion, and (c) NADPH depletion as a function of (□) pH in 100 mM Tris buffer at 25 °C, (■) pH in 100 mM phosphate buffer at 25 °C, (○) phosphate buffer concentration at pH 6.7 and 25 °C, and (●) temperature in 250 mM phosphate buffer at pH 6.7. A table of these rates can be found in Supplemental materials.

buffers, yielding maxima at pH 6.7, while r_{7HCC} exhibited clearly distinct behavior in Tris and phosphate buffers. In Tris-buffered systems, r_{7HCC} increased with decreasing pH down to the lowest assayed pH of 7.1. In phosphate buffered systems, r_{7HCC} exhibited a maximum at pH 7.7.

A strong correlation was observed between $-r_{NADPH}$ and $-r_{EOMCC}$ as a function of both temperature and buffer concentration, indicating that coupling was not significantly changed by these parameters (Fig. 5a). Similarly, the correlation between $-r_{EOMCC}$ and r_{7HCC} indicates that these parameters also did not alter regioselectivity (Fig. 5c). These correlations, showing constant selectivity, contrast with the 6-fold change in activity observed with a variation in temperature and buffer concentration at pH 6.7. The selectivity results are illustrated in Scheme 1 where 7.9% of the reducing equivalents from NADPH were used for coupled catalysis and 1.7% of the overall reducing equivalents or 21.7% of the depleted EOMCC was used to generate 7HCC via O-dealkylation. Conversely, despite the qualitatively similar behavior of $-r_{EOMCC}$ and $-r_{NADPH}$ as a function of buffer type and pH, much weaker correlations were observed for both coupling and regioselectivity as a function of these parameters (Fig. 5b and d). Coupling and regioselectivity varied by 14.4% and 21.6%, respectively. It is important to mention that standard assays containing known amounts of all three fluorophores indicated that the fluorescence responses are not inherently correlated (data not shown). Thus the selectivity trends found in this study are not a result of spurious correlations.

Discussion

Medium engineering offers a useful tool for the investigation of P450 function because a tunable range of P450 responses can be accessed by simply varying the reaction conditions. The practical utility and potential generality of medium engineering has been demonstrated by the large rate increases achieved with optimized P450 reconstitution procedures [6]. The current study seeks to investigate the connection between environment and P450 selectivity using a novel method to simultaneously measure activity, coupling, and regioselectivity.

LCMS analysis verified the presence of multiple coupled products and identified three product peaks. MS/MS analysis revealed an intact ethoxymethoxy moiety on the product eluting at 18.9 min indicating this product is generated via a distinct mechanism from the O-dealkylation product, 7HCC. Furthermore, the mass and formula of the m/z +236 product are consistent with a P450 mediated 3,4-epoxidation followed by a ring opening and decarboxylation similar to the reaction of CYP1A2 with coumarin [26,27]. Interestingly, another product eluting over 11 min later at 30.5 min was identified with a major peak in negative mode LCMS at m/z -207 and a minor peak at m/z -234. This product could not be captured in LCMS/MS analysis; nonetheless, the mass is also consistent with an epoxidation and decarboxylation reaction generating the m/z -234 product that presumably fragments during ionization to form the major m/z -207 peak. Although, the +236 and -234 products exhibit different elution times and different ionization behavior, their similar masses suggest that they may arise from the decarboxylation of a common intermediate generated from a common substrate-binding mode. Overall, however, the MS/MS data indicate the presence of two distinct products that are produced from at least two catalytically relevant binding modes for EOMCC in the CYP1A2 active site. Thus, the regioselectivity determined in this system reflects the relative binding of EOMCC in multiple orientations and the oxidation of multiple sites on the substrate. The presence of multiple binding orientations, indicated by the oxidation of multiple sites on the molecule, is typical of CYP1A2 substrates with caffeine [28] and phenacetin [29] being well-studied examples.

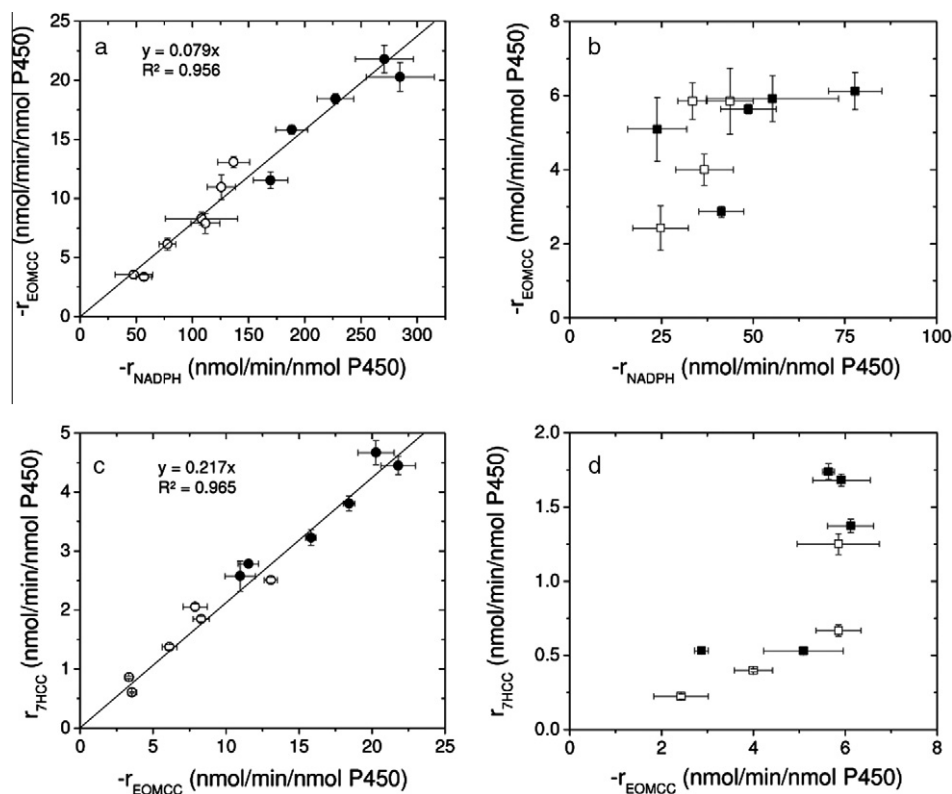
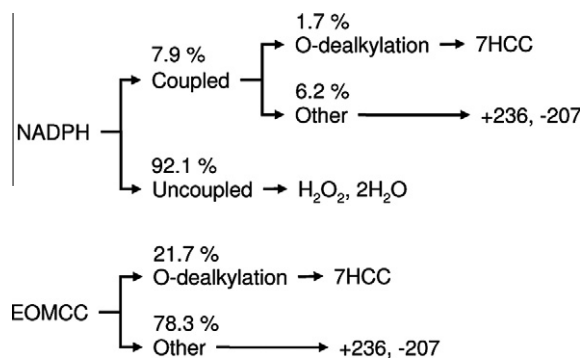


Fig. 5. Correlation of the initial rate of EOMCC depletion, $-r_{\text{EOMCC}}$, with the initial rate of NADPH depletion, $-r_{\text{NADPH}}$, depicting the coupling efficiency (a and b), and of the initial rate of 7HCC generation, r_{7HCC} , with the initial rate of EOMCC depletion, $-r_{\text{EOMCC}}$, depicting the regioselectivity (c and d). The data are from reactions varying the temperature (●) and phosphate buffer concentration (○), and the phosphate pH (■) and Tris pH (□). A table of these selectivity data can be found in [Supplemental materials](#).



Scheme 1. Selectivity of electron (upper) and substrate (lower) utilization in the oxidation of EOMCC by CYP1A2 in pH 6.7 phosphate buffer.

By varying the buffer type, buffer concentration, pH, and temperature in the CYP1A2 oxidation of EOMCC, a 10-fold range of rates was accessed with the highest activity found at pH 6.7 in 250 mM phosphate buffer at 45 °C. Ionic strength is typically varied by varying the buffer concentration, with maximum product-generation rates occurring between 50 and 300 mM [5,6]. Although exceptions have been found for this trend [5], all measured rates in the present study increased with increasing phosphate buffer concentration to a maximum between 250 and 375 mM potassium phosphate. An increase in the measured rates was also observed with temperature between 25 °C and 45 °C, the highest temperature setting available on the instrument. The denaturation temperature of human CYP1A2 in reconstituted membranes reportedly varied with membrane composition between 40 °C and 50 °C [30]. This matched the behavior observed

in the present work where the measured rates showed signs of leveling off at 45 °C.

The measured r_{7HCC} was higher in phosphate than in Tris-buffered systems. Similarly, Mäenpää et al. reported higher product-generation rates in phosphate versus Tris-buffered systems for the midazolam hydroxylation of human liver microsomes [16]. Other studies, however, have shown similar P450 activity in different buffers. For example, the 7-pentoxoresorufin O-dealkylation activity of rabbit CYP1A2 was comparable in sodium phosphate, potassium acetate, and HEPES [31]. Interestingly, $-r_{\text{NADPH}}$ and $-r_{\text{EOMCC}}$ showed similar behavior in phosphate and Tris-buffered systems, demonstrating that buffer type can alter both the rate of product generation and of substrate depletion independently. Since all three measured rates increased similarly with increasing ionic strength, as varied by the phosphate buffer concentration, the inherently larger ionic strength of phosphate compared to Tris is not an adequate argument to explain the different behavior of r_{7HCC} compared to $-r_{\text{EOMCC}}$ and $-r_{\text{NADPH}}$ in these two buffers. P450 reactions are also known to be differentially affected by pH with different product generation optima for different isoform/substrate combinations [14,32,33]. The current study extends this result to show that substrate depletion and product generation can exhibit disparate pH optima.

A strong correlation was observed between $-r_{\text{EOMCC}}$ and $-r_{\text{NADPH}}$ as a function of temperature and phosphate buffer concentration (Fig. 5a) indicating that coupling is not significantly affected by these variables. CYP1A2 oxidation of EOMCC was 92.1% uncoupled for all buffer concentrations and temperatures at pH 6.7. Similarly high uncoupling percentages have been found for the CYP1A2 oxidation of phenacetin [29,34] and of 7-ethoxycoumarin [35] and for other human P450 enzymes [36–38]. A much weaker correlation between $-r_{\text{EOMCC}}$ and $-r_{\text{NADPH}}$ was found as a function of buffer type

and pH (Fig. 5b) indicating that coupling is altered by these variables. To the best of our knowledge this is the first investigation of P450 coupling as a function of buffer type, pH, or temperature. However Schenkman et al. observed an increase in the coupling of the benzphetamine N-demethylation activity of CYP2B4 enriched rabbit liver microsomes with increasing phosphate buffer concentration [22]. This observation contrasts with our own data where buffer concentration did not alter coupling, suggesting that P450 coupling may be differentially regulated by reaction conditions for different P450 systems.

Similarly, regioselectivity was also not significantly altered by temperature or phosphate buffer concentration (Fig. 5c). It was found that 21.7% of the oxidized EOMCC was used to generate the O-dealkylation product 7HCC in pH 6.7 phosphate solution. While no previous study has investigated the effect of temperature on regioselectivity, similar trends with buffer concentration have been observed [14,16]. Buffer concentration did not alter the ratio of several testosterone metabolites from purified rat CYP2A1, CYP2B1, and CYP2C11 [14] or of midazolam metabolites from human liver microsomes [16], consistent with our findings that regioselectivity was insensitive to buffer concentration. However, a change in regioselectivity with pH was reported for the oxidation of testosterone by rat CYP2A1, CYP2B1, and CYP2C11 [14] and for cyclosporine metabolism of human CYP3A4 [15]. Likewise, our results revealed a change in regioselectivity with pH and additionally with buffer type. In light of previous literature on several P450 isoforms and substrates, these data suggest that ionic strength, as varied by buffer concentration, may generally affect the activity of a P450 reaction but not the regioselectivity, while pH may affect both. However, further work with additional P450 isoforms and substrates is needed to confirm this conclusion.

It is relevant to emphasize that 7HCC is a minor product in the overall oxidation of EOMCC by CYP1A2. This low regioselectivity toward O-dealkylation suggests that studies employing 7-alkoxy-3-cyanocoumarin substrates as convenient fluorescent probes for CYP1A2 activity are measuring only a fraction of the reaction products. A further elaboration of the product profile of commonly used coumarin substrates would be a valuable contribution to the literature, especially in light of our current finding that 7HCC accounts for only 21.7% of the substrate depletion.

Because regioselectivity and coupling are governed by enzyme–substrate binding interactions and neither temperature nor buffer concentration altered regioselectivity or coupling, it follows that these parameters do not alter the enzyme–substrate binding interactions. Variations in P450 function with buffer concentration have been previously attributed to the resulting variation in ionic strength and not to specific effects of phosphate ions [5,14,16,22,39]. Although ion-specific effects are known in P450 systems [7,40,41], the correlation of phosphate buffer effects with ionic strength effects is supported by the similar activity trends observed in the CYP1A2 de-ethylation of 7-ethoxyresorufin and 7-ethoxycoumarin as a function of phosphate buffer and sodium chloride concentration [39]. Variations in P450 function with ionic strength have been attributed to an alteration of the P450–reductase interaction [5,22] or the heteromeric oligomerization state [31,42], both of which have been shown to be mediated by ionic interactions [31,42–44]. In addition, the reduction of cytochrome c by P450 reductase, studied as a function of pH and ionic strength, yielded activity maxima at pH 7.5 [45] and an ionic strength of 500 mM [46], similar to the behavior observed in the current work. It is conceivable that selectivity is regulated by the enzyme–substrate binding interaction, which controls substrate positioning, while activity is regulated by the P450–reductase interaction, which controls the flow of electrons to the P450.

Ionic strength, as varied by sodium chloride concentration, has been shown to alter the structure of rabbit CYP1A2 as measured by

circular dichroism [39]. It is interesting that this change in structure could accompany a large change in activity without also perturbing the active site and altering the substrate binding interactions relevant to selectivity. Schrag et al., however, observed constant selectivity in the presence of a structural perturbation of the active site in the CYP3A4 metabolism of triazolam. Regioselectivity was unaffected by a change in active site topography induced by magnesium ions [17]. Overall, it is clear that more work is needed to understand the complex interactions between environmental parameters and P450 function.

In conclusion, mass spectrometry was used to confirm the existence of multiple coupled catalytic modes for the CYP1A2 oxidation of EOMCC in addition to the standard uncoupled modes. An *in situ* optical method was developed to monitor the activity and selectivity of human drug metabolizing enzymes and demonstrated on a cyanocoumarin substrate. This method is anticipated to be a useful tool for protein engineering studies seeking to understand and control the influence of reaction conditions on P450 function. While the activity of CYP1A2 in this work was found to vary over 10-fold as a function of buffer type, buffer concentration, pH, and temperature, the regioselectivity and coupling efficiency were effectively constant with buffer concentration and temperature but varied with buffer type and pH. Future work will investigate the generality of these results with other P450 isoforms with the aim of developing general heuristics relating P450 selectivity and environmental parameters.

Acknowledgments

We thank Rita Nichiporuk and Ulla Anderson for assistance with the mass spectrometry experiments and data interpretation, and Jessica Ryan and Elizabeth Schneider for helpful discussions. This work was supported by the National Science Foundation and the National Institutes of Health.

Appendix A. Supplementary data

Supplementary data associated with this article can be found, in the online version, at doi:10.1016/j.abb.2010.10.002.

References

- [1] P.R. Ortiz de Montellano, Cytochrome P450: Structure, Mechanism, and Biochemistry, Plenum Press, New York, 2005.
- [2] M.K. Julsing, S. Cornelissen, B. Buhler, A. Schmid, *Curr. Opin. Chem. Biol.* 12 (2008) 177–186.
- [3] L.C. Wienkers, T.G. Heath, *Nat. Rev. Drug Discov.* 4 (2005) 825–833.
- [4] E.M.J. Gillam, T. Baba, B.R. Kim, S. Ohmori, F.P. Guengerich, *Arch. Biochem. Biophys.* 305 (1993) 123–131.
- [5] H. Yamazaki, E.M.J. Gillam, M.S. Dong, W.W. Johnson, F.P. Guengerich, T. Shimada, *Arch. Biochem. Biophys.* 342 (1997) 329–337.
- [6] H. Yamazaki, T. Shimada, *Methods Mol. Biol.* 320 (2006) 61–71.
- [7] H. Yamazaki, Y.F. Ueng, T. Shimada, F.P. Guengerich, *Biochemistry* 34 (1995) 8380–8389.
- [8] A. Sigel, H. Sigel, R.K.O. Sigel, *The Ubiquitous Roles of Cytochrome P450 Proteins*, John Wiley & Sons, Ltd., Chichester, U.K., 2007.
- [9] E.M.J. Gillam, *Arch. Biochem. Biophys.* 464 (2007) 176–186.
- [10] R.E. White, M.B. McCarthy, K.D. Egeberg, S.G. Sligar, *Arch. Biochem. Biophys.* 228 (1984) 493–502.
- [11] A. Seifert, S. Tatzel, R.D. Schmid, J. Pleiss, *Proteins: Struct., Funct., Bioinf.* 64 (2006) 147–155.
- [12] M.R. Wester, E.F. Johnson, C. Marques-Soares, P.M. Dansette, D. Mansuy, C.D. Stout, *Biochemistry* 42 (2003) 6370–6379.
- [13] G.T. Miwa, A.Y.H. Lu, *Bioessays* 7 (1987) 215–219.
- [14] B. Gemzik, M.R. Halvorson, A. Parkinson, J. Steroid, *Biochem. Mol. Biol.* 35 (1990) 429–440.
- [15] M. Hermann, E.T. Kase, E. Molden, H. Christensen, *Curr. Drug Metab.* 7 (2006) 265–271.
- [16] J. Maenpaa, S.D. Hall, B.J. Ring, S.C. Strom, S.A. Wrighton, *Pharmacogenetics* 8 (1998) 137–155.
- [17] M.L. Schrag, L.C. Wienkers, *Drug Metab. Dispos.* 28 (2000) 1198–1201.
- [18] P.J. Loida, S.G. Sligar, *Biochemistry* 32 (1993) 11530–11538.

- [19] T.M. Makris, K. von Koenig, I. Schlichting, S.G. Sligar, *Biochemistry* 46 (2007) 14129–14140.
- [20] I.G. Denisov, T.M. Makris, S.G. Sligar, I. Schlichting, *Chem. Rev.* 105 (2005) 2253–2277.
- [21] F.P. Guengerich, *Drug Metab. Rev.* 36 (2004) 159–197.
- [22] J.B. Schenkman, A.I. Voznesensky, I. Jansson, *Arch. Biochem. Biophys.* 314 (1994) 234–241.
- [23] D.M. Stresser, S.D. Turner, A.P. Blanchard, V.P. Miller, C.L. Crespi, *Drug Metab. Dispos.* 30 (2002) 845–852.
- [24] M. Murray, *Curr. Drug Metab.* 1 (2000) 67–84.
- [25] F.P. Guengerich, *Chem. Res. Toxicol.* 14 (2001) 611–650.
- [26] S.L. Born, D. Caudill, K.L. Fliter, M.P. Purdon, *Drug Metab. Dispos.* 30 (2002) 483–487.
- [27] S.L. Born, P.A. Rodriguez, C.L. Eddy, L.D. LehmanMcKeeman, *Drug Metab. Dispos.* 25 (1997) 1318–1323.
- [28] K.A. Regal, K.L. Kunze, R.M. Peter, S.D. Nelson, *Drug. Metab. Dispos.* 33 (2005) 1837–1844.
- [29] C.H. Yun, G.P. Miller, F.P. Guengerich, *Biochemistry* 39 (2000) 11319–11329.
- [30] T. Ahn, C.H. Yun, D.B. Oh, *Biochemistry* 44 (2005) 9188–9196.
- [31] R.W. Kelley, J.R. Reed, W.L. Backes, *Biochemistry* 44 (2005) 2632–2641.
- [32] M. Delaforge, P. Ladam, G. Bouille, J.G. Benarous, M. Jaouen, J.P. Girault, *Chem.-Biol. Interact.* 85 (1992) 215–227.
- [33] J.M. Hutzler, F.J. Powers, M.A. Wynalda, L.C. Wienkers, *Arch. Biochem. Biophys.* 417 (2003) 165–175.
- [34] Q.B. Huang, G.D. Szklarz, *Drug. Metab. Dispos.* 38 (2010) 1039–1045.
- [35] H. Mayuzumi, C. Sambongi, K. Hiroya, T. Shimizu, T. Tateishi, M. Hatano, *Biochemistry* 32 (1993) 5622–5628.
- [36] X.J. Fang, Y. Kobayashi, J.R. Halpert, *FEBS Lett.* 416 (1997) 77–80.
- [37] C.W. Locuson, P.M. Gannett, T.S. Tracy, *Arch. Biochem. Biophys.* 449 (2006) 115–129.
- [38] A. Perret, D. Pompon, *Biochemistry* 37 (1998) 11412–11424.
- [39] C.H. Yun, M. Song, T. Ahn, H. Kim, *J. Biol. Chem.* 271 (1996) 31312–31316.
- [40] J.S. Kim, T. Ahn, S.K. Yim, C.H. Yun, *Biochemistry* 41 (2002) 9438–9447.
- [41] J.S. Kim, C.H. Yun, *Toxicol. Lett.* 156 (2005) 341–350.
- [42] R.W. Kelley, D.M. Cheng, W.L. Backes, *Biochemistry* 45 (2006) 15807–15816.
- [43] D.R. Davydov, A.A. Kariakin, N.A. Petushkova, J.A. Peterson, *Biochemistry* 39 (2000) 6489–6497.
- [44] W.L. Backes, R.W. Kelley, *Pharmacol. Ther.* 98 (2003) 221–233.
- [45] D.S. Sem, C.B. Kasper, *Biochemistry* 32 (1993) 11539–11547.
- [46] D.S. Sem, C.B. Kasper, *Biochemistry* 34 (1995) 12768–12774.